Behavioural Brain Research 293 (2015) 189–197

Contents lists available at ScienceDirect

Behavioural Brain Research

journal homepage: www.elsevier.com/locate/bbr

Research report

Conditioned medium from the stem cells of human dental pulp improves cognitive function in a mouse model of Alzheimer's disease

Tsuneyuki Mita[a], Yoko Furukawa-Hibi[b], Hideyuki Takeuchi[c], Hisashi Hattori[a], Kiyofumi Yamada[b], Hideharu Hibi[a], Minoru Ueda[a], Akihito Yamamoto[a,*]

[a] Department of Oral and Maxillofacial Surgery, Nagoya University Graduate School of Medicine, 65 Tsurumai-cho, Showa-ku, Nagoya 466-8550, Japan
[b] Department of Neuropsychopharmacology and Hospital Pharmacy, Nagoya University Graduate School of Medicine, 65 Tsurumai-cho, Showa-ku, Nagoya 466-8550, Japan
[c] Department of Neuroimmunology, Research Institute of Environmental Medicine, Nagoya University, Furo-cho, Chikusa-ku, Nagoya 464-8601, Japan

HIGHLIGHTS

- Intranasal administration of SHED-CM improves cognition in a mouse model of AD.
- SHED-CM converts the pro-inflammatory AD environment to an anti-inflammatory one.
- SHED-CM induces the accumulation of M2 microglia in the mouse AD brain.
- SHEDs secrete multiple factors beneficial for the treatment of AD.

ARTICLE INFO

Article history:
Received 28 January 2015
Received in revised form 17 July 2015
Accepted 18 July 2015
Available online 22 July 2015

Keywords:
Alzheimer's disease
Dental pulp stem cells
Stem cell-conditioned medium
Microglia
Intranasal administration

ABSTRACT

Alzheimer's disease (AD) is a progressive, neurodegenerative disease characterized by a decline in cognitive abilities and the appearance of β-amyloid plaques in the brain. Although the pathogenic mechanisms associated with AD are not fully understood, activated microglia releasing various neurotoxic factors, including pro-inflammatory cytokines and oxidative stress mediators, appear to play major roles. Here, we investigated the therapeutic benefits of a serum-free conditioned medium (CM) derived from the stem cells of human exfoliated deciduous teeth (SHEDs) in a mouse model of AD. The intranasal administration of SHEDs in these mice resulted in substantially improved cognitive function. SHED-CM contained factors involved in multiple neuroregenerative mechanisms, such as neuroprotection, axonal elongation, neurotransmission, the suppression of inflammation, and microglial regulation. Notably, SHED-CM attenuated the pro-inflammatory responses induced by β-amyloid plaques, and generated an anti-inflammatory/tissue-regenerating environment, which was accompanied by the induction of anti-inflammatory M2-like microglia. Our data suggest that SHED-CM may provide significant therapeutic benefits for AD.

1. Introduction

Alzheimer's disease (AD) is a progressive neurodegenerative disease, characterized by the deterioration of cognitive function associated with the deposition of β-amyloid (Aβ) peptides in the brain [1–4]. Aβ peptides are liberated from larger transmembrane amyloid precursor proteins [5] and generate Aβ_{1-42}/Aβ_{1-40} peptides [2–4]. However, the accurate mechanisms of Aβ-induced neurotoxicity and neuroinflammation are not obviously understood. Previous reports showed that a mouse model of an intracerebroventricular (i.c.v.) injection of Aβ1 – 40 peptide significantly impaired memory acquisition, but not memory retrieval, that resembled the episodic anterograde memory deficit observed in the early phases of AD [6,7]. Thus, the single injection of Aβ1 – 40 peptide into the mouse can be an usefulness for the investigation of molecular mechanisms underlying Aβ peptide toxicity, including the microglial activation and oxidative stress, neuroinflammation and synaptic deficits that lead to cognitive impairments [6].

In AD, elevated levels of Aβ peptides form amyloid plaques that induce the differentiation of M1-type pro-inflammatory microglia, which release high levels of cytokines, glutamate, reactive oxygen species [8] and nitric oxide (NO) [2,9–11]. The resulting oxida-

* Corresponding author. Fax: +81 527 441 978.
E-mail address: akihito@med.nagoya-u.ac.jp (A. Yamamoto).

http://dx.doi.org/10.1016/j.bbr.2015.07.043
0166-4328/

tive stress accelerates the generation of 3-nitrotyrosine (3-NT) in neurons, which suppresses catecholamine synthesis and depresses neuro-synaptic transmission [2,9,12,13]. Recent studies indicate that distinct subpopulations of microglia, including the alternatively activated anti-inflammatory M2 microglia, play pivotal roles in the pathophysiology of AD. M2 microglia counteract the M1-mediated pro-inflammatory environment associated with AD, and promote tissue regeneration by secreting anti-inflammatory cytokines [2,5,10,14], scavenging cellular debris, enhancing axonal elongation and promoting neo-vascularization [15]. Thus, treatments that induce M2 differentiation could provide significant therapeutic benefits for AD.

AD mice have been treated by transplanting various types of stem cells and their derivatives, including human neural stem cells [16], embryonic stem-cell derivatives [17], adult bone-marrow stromal cells (BMSCs) [18], adipogenic stem cells [19] and umbilical cord blood-derived stem cells [20], which have elicited substantial functional recovery through cell-replacement and/or paracrine mechanisms. However, most studies indicate that the cell grafts exhibit poor differentiation and survival in mouse models of AD, suggesting that the functional recovery from AD may be mediated by paracrine mechanisms [16,21,22]. Stem cells are known to secrete a broad repertoire of trophic and immunomodulatory factors, which can be harvested in serum-free conditioned media [23,24]. Recent studies have shown that the factors derived from various types of stem cells have the potential for treating a myriad of intractable diseases [16,21,25]. However, the therapeutic effects of these stem cell-derived factors for AD are largely unknown.

Human adult dental pulp stem cells (DPSCs) and stem cells from human exfoliated deciduous teeth (SHEDs) are self-renewing mesenchymal stem cells (MSCs) residing within the perivascular niche of the dental pulp [26,27]. These cells are thought to originate from the cranial neural crest, which expresses early markers for both MSCs and neural stem cells [26–28], and can differentiate into functional neurons and oligodendrocytes under the appropriate conditions [28–30]. The engraftment of these dental pulp stem cells promotes the functional recovery from various acute and chronic CNS insults through paracrine mechanisms that activate endogenous tissue-repairing activities [28,31–36]. Here, we examined the therapeutic benefits of SHED-CM for mouse AD-like model.

2. Materials and methods

2.1. Animals

Male, 9-week-old imprinting control region (ICR) mice (35–37 g) (Nihon SLC Co., Shizuoka, Japan) were used throughout the study. They were housed in a controlled environment ($23 \pm 1\,^{\circ}C$, $50 \pm 5\%$ humidity), maintained on a 9:00 a.m.– 9:00 p.m. light cycle, and allowed access to food and water. All experiments were performed in accordance with the Guidelines for Animal Experiments of Nagoya University Graduate School of Medicine. All animal procedures and care conformed to the Guidelines for Proper Conduct of Animal Experiments (Science Council of Japan, 2006).

2.2. Treatment and experimental design

The $A\beta_{1-40}$ peptide (obtained from Bachem, Bubendorf, Switzerland) was dissolved in saline as a 1.0 mg/ml stock solution and stored at $-20\,^{\circ}C$ before use. The reverse peptide, $A\beta_{40-1}$ (Bachem) was prepared in the same way and used as a control. Both peptide stock solutions were incubated at $37\,^{\circ}C$ for 4 days, to allow aggregation prior to administration [37]. The peptides were then administered by intracerebroventricular (i.c.v.) injection as described previously [37–41]. Briefly, a microsyringe with a 28-gauge stainless-steel needle, which was 3.0-mm long, was used for all peptide injections. The mice were anesthetized lightly with ether, and the needle was inserted unilaterally 1 mm to the right of the midline point, at an equal distance between the eyes and the ears and perpendicular to the plane of the skull. Thereafter, an i.c.v. injection of 5 μl peptide (5 μg) or vehicle was delivered gradually over 3 min. The mice recovered rapidly and within 1 min of the injection exhibited normal behavior. The administration site was confirmed in preliminary experiments, and neither the insertion of the needle nor the volume of injection significantly influenced the survival, behavioral responses, or cognitive functioning of the mice.

2.3. Isolation of SHEDs from deciduous teeth

Human dental pulp tissues were obtained from clinically healthy, deciduous teeth extracted from patients. The ethics committee of the Nagoya University approved the experimental protocols. The SHEDs were isolated and cultured as previously described [16]. Briefly, the pulp was removed gently and digested for 1 h at $37\,^{\circ}C$ in a solution containing 3 mg/mL collagenase type I and 4 mg/mL dispase. After filtration through 70-mm cell strainers (Falcon; BD Labware), the cells were cultured at $37\,^{\circ}C$ in 5% CO_2 in Dulbecco's modified Eagle's medium (DMEM; Gibco) containing 20% mesenchymal cell growth supplement (Lonza, Inc.) and antibiotics (100 U/mL penicillin, 100 mg/mL streptomycin, and 0.25 mg/mL amphotericin B; Gibco). After primary culture, the cells were sub-cultured at 1×10^4 cells/cm^2 and used in experiments after three to five passages.

2.4. Preparation of SHED-CM, BMSC-CM and Fibro-CM

SHEDs, human bone marrow mesenchymal stem cells (BMSCs) (Lonza, Inc.) and human skin fibroblasts (Fibros) (Health Science Research Resources Bank) were cultured in serum-free DMEM. The conditioned media from SHEDs, BMSCs and Fibros were collected after 48 h of culture and centrifuged at 1500 rpm for 5 min. The supernatants were re-centrifuged at 3000 rpm for 3 min, followed by collection of the second supernatants, which were designated as SHED-CM, BMSC-CM and Fibro-CM, respectively. The protein concentration of each CM supernatant was measured using the BCA protein assay kit (Pierce). The average protein concentration of each CMs was 3 μg/ml. We used most of CM without enrichment or dilution. We found the strong therapeutic effects of this native SHED-CM for the treatment of mouse AD-like model. Furthermore the untreated mouse receiving SHED-CM exhibited no or little adverse events (data not shown).

2.5. Intranasal administration of the CM samples

Twenty-four hours after *i.c.v.* injection of the $A\beta_{1-40}$ peptide (day 1), the mice were anesthetized again with 1.5% isoflurane in O_2. The animals were divided randomly into four groups: the SHED-CM, BMSC-CM, Fibro-CM and DMEM (control) groups ($n = 10$ per group). A total of 50 μL of each of the CM and control samples were administered to the mice intranasally with a Hamilton microsyringe over the course of 10 min, at 2-min intervals. During these procedures, the mouth and opposite nostril were closed. Intranasal administration was performed twice a day for 4 days from days 1 to 4.

2.6. Novel object recognition test

Novel object recognition analysis was performed on days 3 to 5 after the *i.c.v.* injection of $A\beta_{1-40}$ (day 0) [39,41,42]. This method is used to measure of cognitive dysfunction in mouse models of natural aging and AD [43]. A plastic chamber ($35 \times 35 \times 35$ cm) was used

under low light conditions during the light phase of the light/dark cycle. The procedure consisted of three consecutive phases: habituation, acquisition and retention. On day 3 (habituation phase), the mice were individually introduced into the empty chamber and allowed to become familiar with the surroundings for 10 min. On day 4 (acquisition phase), the animals were introduced into the same chamber, which now contained two floor-fixed objects (A and B) placed at equal distances from the center, 15 cm apart from one another and 8 cm from the nearest wall. The mice were allowed to explore the objects for 10 min. On day 5 (retention phase), the mice were allowed to explore the same chamber in the presence of two objects: the familiar object A and a novel object C, which had similar sizes, but different shapes and colors. A recognition index, calculated for each mouse, was expressed as $(TC \times 100)/(TA + TC)$, where TA and TC are the times spent exploring object A and object C at a distance $\leq$1 cm during the retention phase. The time spent exploring the individual objects was recorded by a blinded investigator.

2.7. Sample preparation for Western blot analysis

The cerebral parenchyma was removed 5 days after behavioral testing, placed on an ice-cold glass plate, and immediately frozen and stored at −80 °C. To generate protein extracts, the cerebral parenchyma was homogenized in ice-cold radioimmunoprecipitation assay (RIPA) lysis buffer, supplemented with complete protease inhibitor cocktail tablets (Roche Applied Science, Mannheim, Germany). The homogenates were then centrifuged at 15,000 rpm for 5 min, and the supernatants were collected.

2.8. Western blot analysis

The protein concentrations of the extracts were analyzed by the Lowry method, and then equal amounts (20 μg) of protein were resolved by electrophoresis on Novex 10% Bis–Tris Gels (Life Technologies Corporation, USA), and transferred to a Transfer Stack containing a PVDF membrane (Life Technologies). The membranes were then probed with either an anti-nitrotyrosine mouse monoclonal antibody (Ab) (clone 1A6, Millipore) or an anti-nitric oxide synthase II rabbit polyclonal Ab (Millipore) overnight at 4 °C, or an anti-β-actin goat polyclonal Ab for 1 h at room temperature (Santa Cruz Biotechnology Inc., Santa Cruz, CA, USA). All of the primary antibodies were diluted 1:1000 in 5% BSA in TBS-T. The immunoreactive proteins were detected using Enhanced Chemiluminescence Prime Western Blotting Detection Reagents (GE Healthcare Japan, Tokyo, Japan) and analyzed by ImageQuant LAS 4000 (GE Healthcare Japan). The exposure time for each Western blot was 3 min.

2.9. Real-time PCR

Total RNAs were isolated from the mouse brains 3 h after intranasal administration of the CM samples. RNA concentration was quantified by a spectrophotometer, and RNA integrity was checked by electrophoresis on 1% agarose gels. The reverse transcriptase reactions were performed with Superscript III reverse transcriptase (Invitrogen) using 1 μg of total RNA in a 50-μl reaction volume. Real-time PCR was performed using the THUNDERBIRD SYBR qPCR Mix (Toyobo) and the StepOnePlus Real-Time PCR System (Applied Biosystems). All of the primers were designed using DNADynamo (Blue Tractor Software Ltd) and are shown in Table 1.

Table 1
Primers utilized in RT-PCR.

Gene	Forward sequence (5′–3′)	Reverse sequence(5′–3′)
GAPDH	AACTTTGGCATTGTGGAAGGT	GGATGCAGGGATGATGTTCT
TNF-α	CCCTTTACTCTGACCCCTTTATTGT	TGTCCCAGCATCTTGTGTTTCT
IL-1β	CAGGATGAGGACCCAAGCAC	TCAGACAGCACGAGGCATTT
iNOS	GGCAGGATGAGAAGCTGAGG	CCGCATTAGCACAGAAGCAA
BDNF	TTACCTGGATGCCGCAAACAT	TGACCCACTCGCTAATACTGTC
NGF	TGATCGGCGTACAGGCAGA	GCTGAAGTTTAGTCCAGTGGG
IGF-1	CACATCATGTCGTCTTCACACC	GGAAGCAACACTCATCCACAATG
Arginase 1	AGTGTGGTGCTGGGTGGAGA	TGGTTGTCAGGGGAGTGTTG
Fizz 1	CCAATCCAGCTAACTATCCCTCC	CCAGTCAACGAGTAAGCACAG
Ym 1	TCACTTACACACATGAGCAAGAC	CGGTTCTGAGGAGTAGAGACCA
IL-10	GCTCTTACTGACTGGCATGAG	CGCAGCTCTAGGAGCATGTG

2.10. Neuronal culture and cell viability assay

Primary neuronal cultures were prepared from the cortices of C57BL/6 mice embryos at embryonic day 17 (E17) as described previously [44]. Briefly, cortical fragments were dissociated into single cells in dissociation solution (Sumitomo Bakelite, Akita, Japan), and they were resuspended in nerve culture medium (NCM: Sumitomo Bakelite). Primary neurons were seeded onto 96-well tissue culture plates were coated with 100 μl/ml poly-L-lysine (PLL) at a density of 1×10^4 cells per well or 4 Chamber Polystyrene Vessel Tissue Culture Treated Glass Slide at a density of 5×10^4 cells per well. Cells were incubated at 37 °C in a humidified atmosphere containing 5% CO_2. On 14 days, primary mouse cortical neurons were treated with 20 μM glutamate and SHED-CM for 24 h. Cell viability was determined by the WST assay (Cell Counting Kit-8: DOJINDO). The medium was replaced to 10 v% WST-8 reagent-contained NCM and incubated at 37 °C for 2 h. Then, the absorbance at 450 nm of the formazan produced by living cells was measured using a microplate reader (Spectra Fluor plus, TECAN). Cell viability was calculated relative to the untreated cells.

2.11. Immunohistochemical analysis

On day 1 after the intranasal administration, the mice were perfused transcardially with a 4% paraformaldehyde solution (Nakalai Tesque). The brain was then removed, embedded in OCT compound (Sakura Finetek), and cut into 10-μm-thick sections on a cryostat (Leica). The sections were then permeabilized with 0.1% (v/v) Triton X-100 in PBS for 20 min, blocked with 5% (v/v) bovine serum albumin in PBS for 30 min, and incubated overnight with the following primary antibodies: anti-Iba1 (marker of microglia) goat polyclonal antibody (1:500; Abcam, Inc.) or anti-Ym-1 (marker of M2 type microglia) rabbit polyclonal antibody (1:40; Abcam, Inc.). After the sections were washed, they were incubated for 30 min with the following secondary Abs: anti-goat IgG-Alexa Fluor 546 or anti-rabbit IgG-Alexa Fluor 647, and counterstained with 4′,6-diamidino-2-phenylindole (DAPI; Sigma–Aldrich). Neurons were fixed with 4% paraformaldehyde, blocked, and permeabilized. Neurons were stained with anti-microtubule-associated protein 2 (MAP2: maker of neuron) antibody (1:1000; Merckmillipore, Inc.) followed by the secondary antibody anti-rabbit IgG-Alexa Fluor 647 (1:1000; Invitrogen) and counterstained with Hoechst 33,342 (Molecular Probe). The stained tissue and cell images were captured with a universal fluorescence microscope (BZ9000, Keyence). The average number of Ym-1-positive and Iba1-positive cells per section was determined by counting 90 random, non-overlapping fields at 400X magnification. At least 3 mice per group were examined.

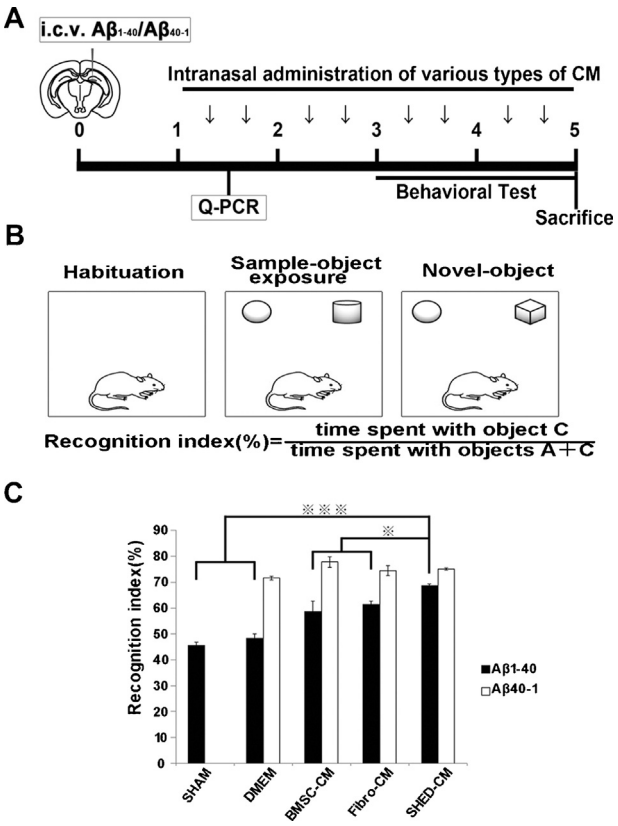

Fig. 1. Intranasal administration of SHED-CM ameliorates the neurological dysfunction of Aβ_{1-40}-injected mice. (A) Experimental protocol. SHED-CM, Fibro-CM, BMSC-CM and DMEM were administered twice a day on days 1 to 4 following the i.c.v. injection of 5 μg Aβ_{1-40} or the control Aβ_{40-1} peptide on day 0. (B) Mice injected with either Aβ_{1-40} or Aβ_{40-1} peptide were subjected to the novel object recognition task on days 3–5. (C) Mice treated with Aβ_{1-40} or Aβ_{40-1} followed by intranasal administration of SHED-CM, BMSC-CM, Fibro-CM, or DMEM were subjected to the novel object recognition task. Values indicate the mean ± SEM; $n = 10$, $^{*}P < 0.05$, $^{***}P < 0.001$.

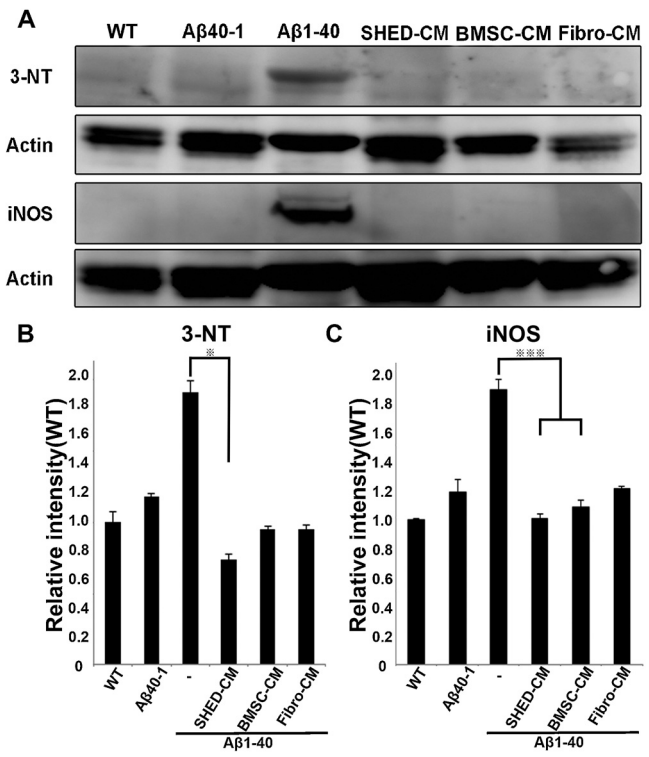

Fig. 2. SHED-CM, Fibro-CM and BMSC-CM inhibit oxidative-nitrosative stress in the cerebral parenchyma of Aβ_{1-40}-injected mice. (A) SHED-CM, Fibro-CM, BMSC-CM and DMEM were administered twice a day on days 1 to 4 following the i.c.v. injection of Aβ_{1-40} on day 0. (B and C) 3-nitrotyrosine (3-NT) and inducible nitric oxide synthase (iNOS) [8] in the cerebral parenchyma were measured by Western blotting on day 5. Quantification of the bands for 3-NT (B) and iNOS (C), normalized to β-actin and expressed as a percentage of the level in the control group. Values indicate the mean ± SEM; $n = 3$, $^{*}P < 0.05$, $^{**}P < 0.01$, $^{***}P < 0.001$.

3. Results

3.1. SHED-CM ameliorates neurological dysfunction in a mouse AD-like model

The goal of this study was to evaluate the therapeutic effects of the factors released from SHEDs on a mouse AD-like model. The conditioned medium [23] from SHEDs, BMSCs and primary human fibroblasts (Fibros) were collected 48 h after culture in DMEM. The primary characteristics of the cells used to generate the CM were described in our previous report [28]. There were no significant differences in the cellular survival of the various cell types following incubation in serum-free media (data not shown). Mice with AD-like neuropathology were generated by the intracerebroventrical (i.c.v.) injection of Aβ_{1-40} oligomers. The resulting neurogenic behaviors were evaluated by the novel object recognition task, and quantified by the recognition index (RI, see Materials and Methods and Fig. 1A and B). Mice receiving the Aβ$_{1-40}$ but not the control, reverse peptide (Aβ_{40-1}) exhibited a significantly reduced RI compared to that of the sham-operated group. The various types of CM were administered intranasally and their effect on cognitive dysfunction was examined. Mice receiving SHED-CM exhibited significantly improved RI, while those receiving BMSC-CM or Fibro-CM exhibited only modestly improved RI (Fig. 1C). The RI of the DMEM group was similar to that of the control mice receiving Aβ_{1-40} injection with no additional treatment. These data demonstrated that SHED-CM improved the cognitive dysfunction associated with mouse AD-like model.

3.2. SHED-CM inhibits the generation of 3-NT

To investigate the mechanism by which SHED-CM improved cognition in mouse AD-like model, the brains of the mice evaluated above were isolated 5 days after behavioral testing, processed as described in Materials and Methods, and then the protein extracts were subjected to immuno-blotting analysis with antibodies to 3-nitrotyrosine (3-NT) or nitric oxide syntheses II [8]. The levels of both 3-NT and iNOS were markedly increased in the Aβ_{1-40}-, but not Aβ_{40-1}-injected mice. Notably, treatment with SHED-CM, BMSC-CM, or Fibro-CM significantly inhibited the generation of both 3-NT and iNOS in AD mice (Fig. 2A–C). These results demonstrated that intranasal administration of the CM from the three cell types similarly suppressed Aβ_{1-40}-induced oxidative stress.

3.3. SHED-CM converts the pro-inflammatory brain environment of the mouse AD-like model to an anti-inflammatory one and increases neurotrophic factor expression

To examine the effect of the various CM samples on the expression of pro-inflammatory cytokines and neurotropic factors involved in the pathophysiology of AD, total RNAs were isolated from mouse brains 3 h after the first intranasal injection and subjected to quantitative RT-PCR analysis. The pro-inflammatory M1 markers (IL-1β, TNF-α and iNOS) were markedly up-regulated in the brains of mice receiving Aβ_{1-40} peptide, whereas subsequent treatment with SHED-CM, BMSC-CM or Fibro-CM similarly

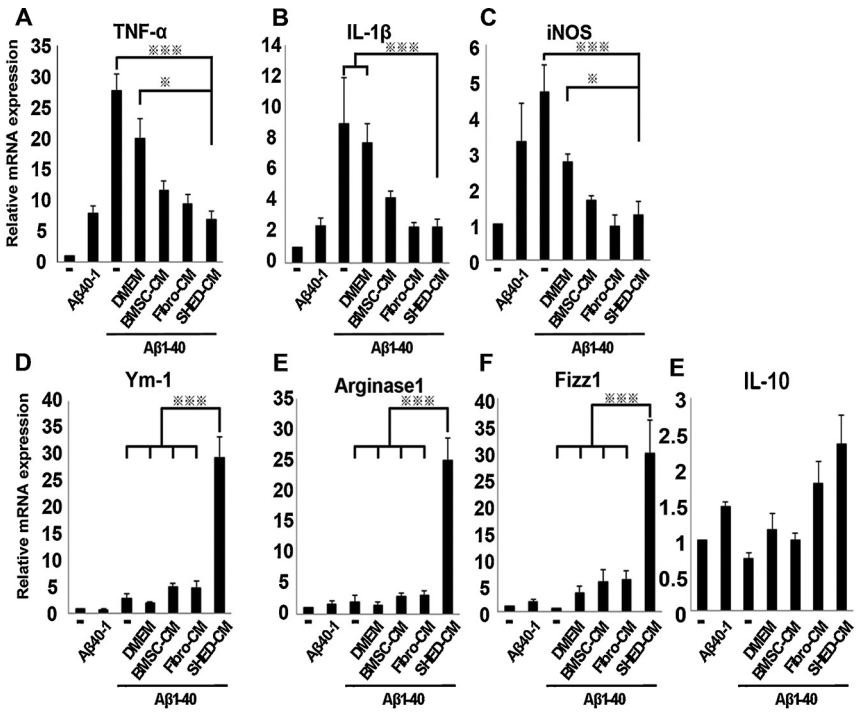

Fig. 3. SHED-CM converts the pro-inflammatory environment of the AD mouse brain to an anti-inflammatory one. (A to G) Levels of the indicated mRNAs in the brains of Aβ_{1-40}-injected mice treated with SHED-CM, Fibro-CM, BMSC-CM and DMEM. Total RNAs were isolated from the cerebral parenchyma 3 h after intranasal administration of the various CM samples and DMEM control. Quantitative real-time PCR was performed to evaluate the expression of pro-inflammatory cytokine mRNAs (*TNF-α* (A), *IL-1β* (B)), *iNOS* (C), M2-type microglia markers (*Ym-1*(D), *Arginase1* (E) and *Fizz1*(F)) and *IL-10*(G). The results are expressed relative to the mRNA levels in the control group. Data are presented as the means ± SEM; $n = 3$, $^{*}P < 0.05$, $^{**}P < 0.01$, $^{***}P < 0.001$.

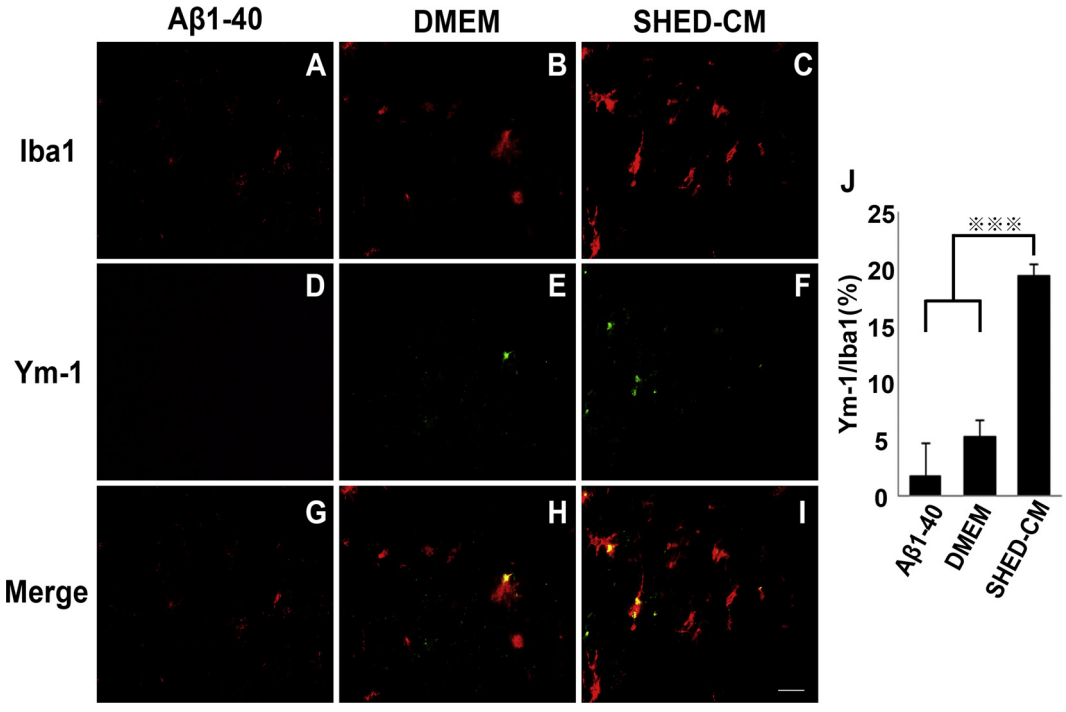

Fig. 4. SHED-CM promotes the accumulation of M2-type microglia in the brain of Aβ_{1-40}-injected mice. Immunohistochemical staining of M2-type microglia 3 h after the intranasal administration of SHED-CM or DMEM into Aβ_{1-40}-injected mice. Immunofluorescence staining of Iba1-positive cells (A,B,C), Ym-1-positive cells (D,E,F), and Iba1/Ym-1-double positive cells (G,H,I). Scale bar: 100 μm. (J) The percentage of Iba1-positive cells that were Ym-1-positive is shown. The results shown represent the average of 3 experiments performed in parallel. Values indicate the mean ± SD; $n = 3$, $^{*}P < 0.05$, $^{**}P < 0.01$, $^{***}P < 0.001$.

suppressed their expression (Fig. 3A–C). In contrast, treatment with SHED-CM, but not BMSC-CM or Fibro-CM, uniquely up-regulated the expression of the anti-inflammatory M2 markers Ym-1, Arginase1 and Fizz1 (Fig. 3D–F). The expressions of a major anti-inflammatory cytokine, IL-10, was also elevated in SHED-CM Group (Fig. 3G). Consistent with these observations, immunohistochemical staining revealed that the number of Ym-1-positive/Iba1-positive M2-like cells was increased in the brains

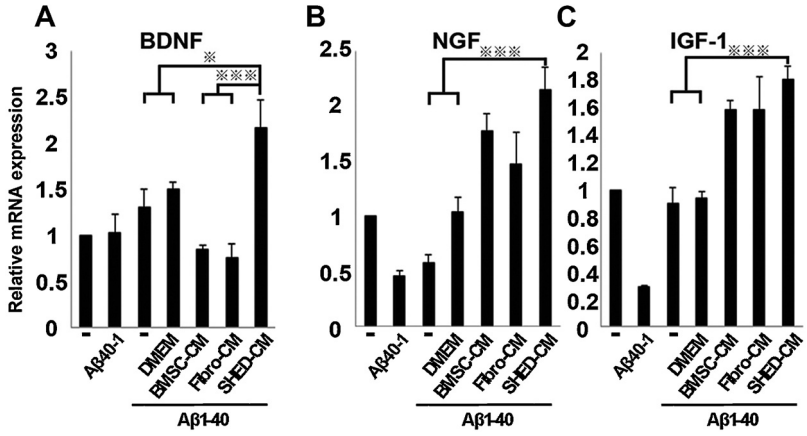

Fig. 5. SHED-CM promotes the expression of multiple neurotrophic factors. (A–C) Levels of the indicated mRNAs in the brain of Aβ_{1-40}-injected mice treated with SHED-CM, Fibro-CM, BMSC-CM or DMEM. Total RNA was isolated from the cerebral parenchyma 3 h after intranasal administration of the various CM samples or control DMEM. Quantitative real-time PCR analysis of *BDNF* (A), *NGF* (B) and *IGF-1* (C). Results are expressed relative to the mRNA level in the control group and are presented as the means ± SEM. $n = 3$, $^{*}P < 0.05$, $^{**}P < 0.01$, $^{***}P < 0.001$.

of SHED-CM-treated mice (Fig. 4). Furthermore, SHED-CM treatment increased the mRNA expression of multiple neurotrophic factors associated with synaptic transmission and/or neuroprotection in AD, including *BDNF*, *NGF* and *IGF* (Fig. 5A–C). Notably, *BDNF* was uniquely upregulated in the brain of SHED-CM-treated mice, whereas *NGF* and *IGF* were upregulated in response to all of the CM samples (Fig. 5). Taken together, these results demonstrated that SHED-CM shifted the M1-type pro-inflammatory microenvironment associated with mouse AD toward the M2-type anti-inflammatory/neuroprotective one.

3.4. Neuroprotective effects of SHED-CM against glutamate neurotoxicity

We next analyzed the neuroprotective effects of SHED-CM against neurotoxicity using primary cerebral neurons isolated from mouse embryos. Stimulation with glutamate reduced number of surviving MAP2-positive neurons (Fig. 6A and C). Treatment with SHED-CM suppressed glutamate-induced neuronal death (Fig. 6B and D). Furthermore, WST-8 assay also revealed that SHED-CM treatment significantly improved cell viability (Fig. 6E). These results demonstrate that SHED-CM exerts neuroprotective effects.

4. Discussion

Numerous studies have reported that the intracerebral engraftment of various types of stem cells improves cognitive impairments associated with mouse AD by paracrine mechanisms [25,45]. However, whether the application of stem cell-derived paracrine factors alone, without the cell graft, would promote significant recovery has been uncertain. Here, we report for the first time, to our knowledge, on the therapeutic benefits of administering stem cell-derived CM for AD. Using the Aβ peptide-induced mouse model of AD, we found that the intranasal administration of SHED-CM was significantly more effective in improving cognitive function than either BMSC-CM or Fibro-CM. SHED-CM treatment converted the pro-inflammatory brain environment associated with AD to an anti-inflammatory one, associated with an altered microglial phenotype. Thus, our data suggest that SHED-CM may provide significant therapeutic benefits for AD.

Recently, we characterized the soluble factors in SHED-CM by cytokine antibody array analysis. SHED-CM contained 48 of the proteins in the array, at levels that were more than 1.5–fold greater than that in DMEM (Matsushita, Y. et al., unpublished observation). By cluster analysis of the 48 proteins, we identified 14 of these proteins that exhibit functional properties that may be beneficial for the treatment of AD, including those involved in inflammation suppression, neuro-protection and apoptosis inhibition, axonal elongation, microglial regulation, and angiogenesis (Table 2). For example, brain derived neurotrophic factor (BDNF) supports neuronal survival and plasticity [46] and is involved in learning and memory formation [47,48], while glial cell line-derived neurotrophic factor [49,49] is neuroprotective [50,51], inhibits microglial activation [52] and promotes axonal regeneration [51,53]. TIMP-1, stem cell factor (SCF) and hepatocyte growth factor (HGF) also exhibit neuroprotective activities [54–56]. MMP-9 reduces the level of pathogenic Aβ oligomers in AD mice and restores synaptic and cognitive deficits in these mice [57], while transforming growth factor-β (TGF-β) modulates microglial activation [58]. The concentrations of these factors in SHED-CM may

Table 2
Ratio > 1.5(vs DMEM).

Anti-inflammation	SHED-CM	BMSC-CM	Fibro-CM
IL-6	2.814524	3.042002	3.86453
TGF-β	1.687249	0.992526	0.997852

Neuro protection/Anti-apoptosis	SHED-CM	BMSC-CM	Fibro-CM
TIMP1	128.2696	110.5529	119.1118
HGF	43.4167	13.13753	1.005414
SCF	6.538547	7.968416	1.504465
BDNF	1.781828	0.882627	0.776783
GDNF	1.599768	0.888424	0.719246
MMP9	1.597813	0.790366	0.859767

Axonal eleongation	SHED-CM	BMSC-CM	Fibro-CM
TIMP2	285.6889	188.8058	281.9644
Decorin	264.8396	248.8142	267.6825
MMP3	7.062882	0.921822	2.047458
SCF	6.538547	7.968416	1.504465

Microglia-related factors	SHED-CM	BMSC-CM	Fibro-CM
MCP-1	57.89063	59.53194	6.842407
HGF	43.4167	13.13753	1.005414
IL-6	2.814524	3.042002	3.86453
TGF-β	1.687249	0.992526	0.997852
GDNF	1.599768	0.888424	0.719246

Angiogenesis	SHED-CM	BMSC-CM	Fibro-CM
HGF	43.4167	13.13753	1.005414
VEGF	7.185871	4.127233	5.244794

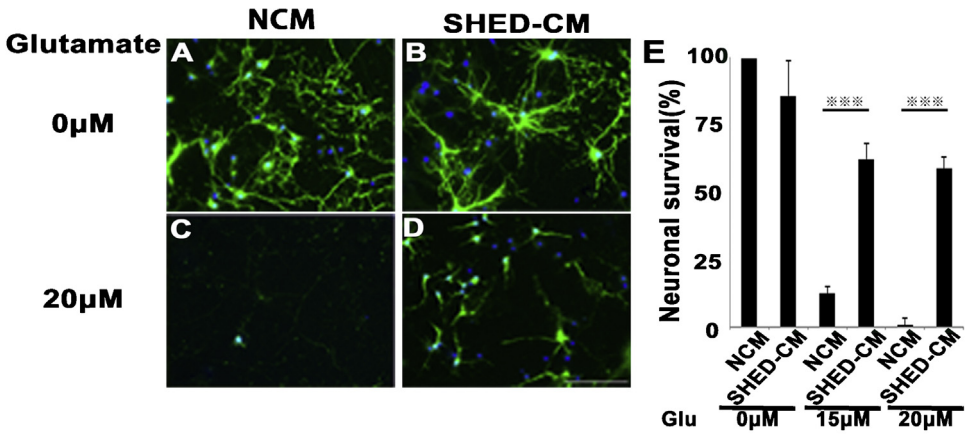

Fig. 6. SHED-CM suppressed glutamate-induced neuronal death. (A-D) Immunohistochemical staining of neurons treated with 20 μM glutamate in NCM or SHED-CM. Neurons and cell nuclei were stained with an anti-MAP-2 antibody (green) and Hoechst 33,342 (blue), respectively. Scale bar: 100 μm. (E) The cell variability was analyzed by WST assay and calculated relative to the untreated cells. Neurons were treated with glutamate (0, 15, 20 μM) in NCM or SHED-CM. Values indicate the mean ± SEM; $n = 6$, $^{***}P < 0.001$. (For interpretation of the references to color in this figure legend, the reader is referred to the web version of this article.)

be quite low; however, we believe that the combinatorial effects of these factors in SHED-CM could provide therapeutic benefits for AD.

Our data suggested that SHED-CM improved the cognitive deficits associated with mouse AD, in part by converting the pro-inflammatory environment of the AD brain to an anti-inflammatory/neuroprotective one. The deposition of Aβ oligomers induces M1-type microglia to generate various neurotoxic mediators, which in turn induce neuronal death and suppress neurotransmission. In contrast, M2-type cells suppress M1-mediated inflammation and secrete multiple neurotrophic factors, which improve neurotransmission [11,59]. Our data showed that treatment with SHED-CM, BMSC-CM or Fibro-CM similarly suppressed the expression of pro-inflammatory cytokines and markers of oxidative-nitrosative stress. In contrast, SHED-CM uniquely activated M2-type microglia, which led to the expression of the mRNA encoding BDNF, a neurotrophin that plays a central role in the synaptic remodeling associated with memory formation in the adult hippocampus. Notably, this neuropathological recovery is reminiscent of that observed in our previous study, in which the intracerebral administration of SHED-CM in mice with a perinatal hypoxia-ischemia-induced brain injury generated an anti-inflammatory microenvironment, reduced tissue loss, and significantly improved the neurological outcome [35]. Thus, our findings collectively suggest that the conversion of a pro-inflammatory/neuro-destructive environment to an anti-inflammatory/neuroprotective one may provide powerful benefits for the treatment of brain injury and neurodegenerative diseases. Our data suggest that the unique immune-regulatory activity exhibited by SHED-CM plays a major role in mediating the recovery of cognitive function.

SHED-CM contained of various type of neuroprotective factors. In our previous studies, we reported that engraftment of SHED or SHED-CM administration into the rat spinal cord injury or ischemic brain injury significantly reduced the number of apoptosis [26,32,33]. Furthermore, SHED-CM suppressed 6-hydroxydopamine-induced cell death and enhanced the neurite growth of cerebellar granule neurons. The trophic activity of SHED improved neurological deficits of Parkinsonian rats [60]. In this study, we showed that SHED-CM protected primary cerebral neurons against glutamate neurotoxicity. Taken together, these results suggest that neuroprotective effects of SHED-CM may provide therapeutic benefits for AD treatment.

Intranasally administered therapeutic molecules are targeted to the central nervous system along the olfactory, trigeminal neural and vascular routes [61,62]. Intranasal administration is a minimally invasive, easily repeatable, and simple procedure. The intranasal administration of IGF-1 achieves significantly higher concentrations in the CNS than intravenous administration [63]. Furthermore, AD mice receiving intranasal administrations of IGF-1 [64], insulin [8], NGF [65] or S14G-Humanin [66] exhibit substantially improved cognitive function. In addition, we previously demonstrated that the intranasal administration of SHED-CM reduced the neurological deficits in a rat model of focal cerebral ischemia [34]. Thus, our current data, taken together with previous findings, suggest that the intranasal administration of SHED-CM may provide a highly efficacious, less invasive therapeutic strategy for neurodegenerative disorders.

5. Conclusion

Here we demonstrated the impressive therapeutic benefits of serum-free CM derived from SHEDs for mouse AD-like model. The multifaceted activities of SHED-CM may provide many neuroreparative effects required for the treatment of cognitive deficits. Notably, we did not observe any adverse effects during the experimental treatment period. Thus, our data suggest that SHED-CM may provide a novel cell-free neuro-reparative therapy for AD.

Acknowledgements

We are grateful to T. Inoue, M. Yamagata and K. Matsubara for their helpful comments and support of this study. We thank the Division of Experimental Animals and Medical Research Engineering, Nagoya University Graduate School of Medicine, for the housing of mice and for microscope maintenance. This work was supported by Grants-in-Aid for Scientific Research on Priority Areas from the Ministry of Education, Culture, Sports, Science, and Technology of Japan, and Grants-in-Aid for the Practical Application of Regenerative Medicine from the Ministry of Health, Labour, and Welfare of Japan.

References

[1] L. Bertram, C.M. Lill, R.E. Tanzi, The genetics of Alzheimer disease: back to the future, Neuron 68 (2010) 270–281.
[2] M. Citron, Alzheimer's disease: strategies for disease modification, Nat. Rev. Drug Discov. 9 (2010) 387–398.
[3] Y.D. Huang, L. Mucke, Alzheimer mechanisms and therapeutic strategies, Cell 148 (2012) 1204–1222.

[4] A.M. Swomley, S. Forster, J.T. Keeney, J. Triplett, Z. Zhang, R. Sultana, Abeta, oxidative stress in Alzheimer disease: evidence based on proteomics studies, Biochim. Biophys. Acta 2014 (1842) 1248–1257.
[5] S.H. Appel, W. Zhao, D.R. Beers, J.S. Henkel, The microglial-motoneuron dialogue in ALS, Acta Myol. 30 (2011) 4–8.
[6] V.V. dos Santos, D.B. Santos, G. Lach, A.L.S. Rodrigues, M. Farina, T.C.M. De Lima, et al., Neuropeptide Y. (NPY) prevents depressive-like behavior, spatial memory deficits and oxidative stress following amyloid-beta (A beta(1-40)) administration in mice, Behav. Brain Res. 244 (2013) 107–115.
[7] L.V. Colom, M.T. Castaneda, D. Aleman, A. Touhami, Memantine protects cholinergic and glutamatergic septal neurons from A beta(1-40)-induced toxicity, Neurosci Lett. 541 (2013) 54–57.
[8] S. Craft, L.D. Baker, T.J. Montine, S. Minoshima, G.S. Watson, A. Claxton, et al., Intranasal insulin therapy for Alzheimer disease and amnestic mild cognitive impairment: a pilot clinical trial, Arch. Neurol. 69 (2012) 29–38.
[9] V. Chauhan, A. Chauhan, Oxidative stress in Alzheimer's disease, Pathophysiology 13 (2006) 195–208.
[10] M.M. Varnum, T. Ikezu, The classification of microglial activation phenotypes on neurodegeneration and regeneration in Alzheimer's disease brain, Arch. Immunol. Ther. Exp. (Warsz) 60 (2012) 251–266.
[11] C.H. Latta, H.M. Brothers, D.M. Wilcock, Neuroinflammation in Alzheimer's disease; A source of heterogeneity and target for personalized therapy, Neuroscience (2015), in press.
[12] I. Benilova, E. Karran, B. De Strooper, The toxic Abeta oligomer and Alzheimer's disease: an emperor in need of clothes, Nat. Neurosci. 15 (2012) 349–357.
[13] K. Dasuri, L. Zhang, J.N. Keller, Oxidative stress, neurodegeneration, and the balance of protein degradation and protein synthesis, Free Radic. Biol. Med. 62 (2013) 170–185.
[14] V.E. Miron, R.J. Franklin, Macrophages and CNS remyelination, J. Neurochem. 130 (2014) 165–171.
[15] S. David, A. Kroner, Repertoire of microglial and macrophage responses after spinal cord injury, Nat. Rev. Neurosci. 12 (2011) 388–399.
[16] M. Blurton-Jones, M. Kitazawa, H. Martinez-Coria, N.A. Castello, F.J. Muller, J.F. Loring, et al., Neural stem cells improve cognition via BDNF in a transgenic model of Alzheimer disease, Proc. Natl. Acad. Sci. U. S. A. 106 (2009) 13594–13599.
[17] F.H. Moghadam, H. Alaie, K. Karbalaie, S. Tanhaei, M.H.N. Esfahani, H. Baharvand, Transplantation of primed or unprimed mouse embryonic stem cell-derived neural precursor cells improves cognitive function in Alzheimerian rats, Differentiation 78 (2009) 59–68.
[18] J.K. Lee, H.K. Jin, J.S. Bae, Bone marrow-derived mesenchymal stem cells reduce brain amyloid-beta deposition and accelerate the activation of microglia in an acutely induced Alzheimer's disease mouse model, Neurosci. Lett. 450 (2009) 136–141.
[19] S. Kim, K.A. Chang, J. Kim, H.G. Park, J.C. Ra, H.S. Kim, et al., The preventive and therapeutic effects of intravenous human adipose-derived stem cells in Alzheimer's disease mice, Plos One 7 (2012) e45757.
[20] H.J. Lee, J.K. Lee, H. Lee, J.E. Carter, J.W. Chang, W. Oh, et al., Human umbilical cord blood-derived mesenchymal stem cells improve neuropathology and cognitive impairment in an Alzheimer's disease mouse model through modulation of neuroinflammation, Neurobiol. Aging 33 (2012) 588–602.
[21] H. Yang, Z. Xie, L. Wei, H. Yang, S. Yang, Z. Zhu, et al., Human umbilical cord mesenchymal stem cell-derived neuron-like cells rescue memory deficits and reduce amyloid-beta deposition in an AbetaPP/PS1 transgenic mouse model, Stem Cell Res. Therapy 4 (2013) 76.
[22] J.K. Lee, H.K. Jin, S. Endo, E.H. Schuchman, J.E. Carter, J.S. Bae, Intracerebral transplantation of bone marrow-derived mesenchymal stem cells reduces amyloid-beta deposition and rescues memory deficits in Alzheimer's disease mice by modulation of immune responses, Stem Cells 28 (2010) 329–343.
[23] L.A. MacMillan-Crow, J.P. Crow, J.A. Thompson, Peroxynitrite-mediated inactivation of manganese superoxide dismutase involves nitration and oxidation of critical tyrosine residues, Biochemistry 37 (1998) 1613–1622.
[24] S.H. Ranganath, O. Levy, M.S. Inamdar, J.M. Karp, Harnessing the mesenchymal stem cell secretome for the treatment of cardiovascular disease, Cell Stem Cell 10 (2012) 244–258.
[25] M. Li, K. Guo, S. Ikehara, Stem cell treatment for Alzheimer's disease, Int. J. Mol. Sci. 15 (2014) 19226–19238.
[26] S. Gronthos, M. Mankani, J. Brahim, P.G. Robey, S. Shi, Postnatal human dental pulp stem cells (DPSCs) in vitro and in vivo, Proc. Natl. Acad. Sci. U. S. A. 97 (2000) 13625–13630.
[27] M. Miura, S. Gronthos, M. Zhao, B. Lu, L.W. Fisher, P.G. Robey, et al., SHED: stem cells from human exfoliated deciduous teeth, Proc. Natl. Acad. Sci. U. S. A. 100 (2003) 5807–5812.
[28] K. Sakai, A. Yamamoto, K. Matsubara, S. Nakamura, M. Naruse, M. Yamagata, et al., Human dental pulp-derived stem cells promote locomotor recovery after complete transection of the rat spinal cord by multiple neuro-regenerative mechanisms, JCI 122 (2012) 80–90.
[29] A. Arthur, G. Rychkov, S. Shi, S.A. Koblar, S. Gronthos, Adult human dental pulp stem cells differentiate toward functionally active neurons under appropriate environmental cues, Stem Cells 26 (2008) 1787–1795.
[30] M. Király, B. Porcsalmy, A. Pataki, K. Kádár, M. Jelitai, B. Molnár, et al., Simultaneous PKC. and cAMP activation induces differentiation of human dental pulp stem cells into functionally active neurons, Neurochem. Int. 55 (2009) 323–332.
[31] Z. Taghipour, K. Karbalaie, A. Kiani, A. Niapour, H. Bahramian, M.H. Nasr-Esfahani, et al., Transplantation of undifferentiated and induced human exfoliated deciduous teeth-derived stem cells promote functional recovery of rat spinal cord contusion injury model, Stem Cells Dev 21 (2012) 1794–1802.
[32] F.M. de Almeida, S.A. Marques, S. Ramalho Bdos, R.F. Rodrigues, D.V. Cadilhe, D. Furtado, et al., Human dental pulp cells: a new source of therapy in a mouse model of compressive spinal cord injury, J. Neurotrauma. 28 (2011) 1939–1949.
[33] W.K. Leong, T.L. Henshall, A. Arthur, K.L. Kremer, M.D. Lewis, S.C. Helps, et al., Human adult dental pulp stem cells enhance poststroke functional recovery through non-neural replacement mechanisms, Stem Cells Transl. Med. 1 (2012) 177–187.
[34] T. Inoue, M. Sugiyama, H. Hattori, H. Wakita, T. Wakabayashi, M. Ueda, Stem cells from human exfoliated deciduous tooth-derived conditioned medium enhance recovery of focal cerebral ischemia in rats, Tissue Eng. Part A 19 (2013) 24–29.
[35] M. Yamagata, A. Yamamoto, E. Kako, N. Kaneko, K. Matsubara, K. Sakai, et al., Human dental pulp-derived stem cells protect against hypoxic-ischemic brain injury in neonatal mice, Stroke (2013) 551–554.
[36] A. Yamamoto, K. Sakai, K. Matsubara, F. Kano, M. Ueda, Multifaceted neuro-regenerative activities of human dental pulp stem cells for functional recovery after spinal cord injury, Neurosci. Res. 78 (2014) 16–20.
[37] T. Alkam, A. Nitta, H. Mizoguchi, A. Itoh, R. Murai, T. Nagai, et al., The extensive nitration of neurofilament light chain in the hippocampus is associated with the cognitive impairment induced by amyloid beta in mice, J. Pharmacol. Exp. Ther. 327 (2008) 137–147.
[38] T. Maurice, B.P. Lockhart, A. Privat, Amnesia induced in mice by centrally administered beta-amyloid peptides involves cholinergic dysfunction, Brain Res. 706 (1996) 181–193.
[39] T. Alkam, A. Nitta, H. Mizoguchi, A. Itoh, T. Nabeshima, A natural scavenger of peroxynitrites, rosmarinic acid, protects against impairment of memory induced by Abeta(25–35), Behav. Brain Res. 180 (2007) 139–145.
[40] T. Alkam, A. Nitta, Y. Furukawa-Hibi, M. Niwa, H. Mizoguchi, K. Yamada, et al., Oral supplementation with Leu-Ile, a hydrophobic dipeptide, prevents the impairment of memory induced by amyloid beta in mice via restraining the hyperphosphorylation of extracellular signal-regulated kinase, Behav. Brain Res. 210 (2010) 184–190.
[41] Y. Furukawa-Hibi, T. Alkam, A. Nitta, A. Matsuyama, H. Mizoguchi, K. Suzuki, et al., Butyrylcholinesterase inhibitors ameliorate cognitive dysfunction induced by amyloid-beta peptide in mice, Behav. Brain Res. 225 (2011) 222–229.
[42] T. Nagai, K. Takuma, H. Kamei, Y. Ito, N. Nakamichi, D. Ibi, et al., Dopamine D1 receptors regulate protein synthesis-dependent long-term recognition memory via extracellular signal-regulated kinase 1/2 in the prefrontal cortex, Learn. Mem. 14 (2007) 117–125.
[43] A. Nitta, A. Itoh, T. Hasegawa, T. Nabeshima, beta-Amyloid protein-induced Alzheimer's disease animal model, Neurosci. Lett. 170 (1994) 63–66.
[44] H. Takeuchi, T. Mizuno, G. Zhang, J. Wang, J. Kawanokuchi, R. Kuno, et al., Neuritic beading induced by activated microglia is an early feature of neuronal dysfunction toward neuronal death by inhibition of mitochondrial respiration and axonal transport, J. Biol. Chem. 280 (2005) 10444–10454.
[45] S.S. Choi, S.R. Lee, S.U. Kim, H.J. Lee, Alzheimer's disease and stem cell therapy, Exp. Neurobiol. 23 (2014) 45–52.
[46] B. Lu, W. Gottschalk, Modulation of hippocampal synaptic transmission and plasticity by neurotrophins, Prog. Brain Res. 128 (2000) 231–241.
[47] Y. Lu, K. Christian, B.B.D.N.F. Lu, A key regulator for protein synthesis-dependent LTP and long-term memory, Neurobiol. Learn. Mem. 89 (2008) 312–323.
[48] T. Ozawa, K. Yamada, Y. Ichitani, B.D.N.F. Hippocampal, treatment facilitates consolidation of spatial memory in spontaneous place recognition in rats, Behav. Brain Res. 263 (2014) 210–216.
[49] J.G. Nutt, K.J. Burchiel, C.L. Comella, J. Jankovic, A.E. Lang, E.R. Laws Jr., et al., Randomized, double-blind trial of glial cell line-derived neurotrophic factor (GDNF) in PD, Neurology 60 (2003) 69–73.
[50] S.J. Allen, J.J. Watson, D.K. Shoemark, N.U. Barua, N.K. Patel, GDNF, NGF. and BDNF as therapeutic options for neurodegeneration, Pharmacol. Therapeut. 138 (2013) 155–175.
[51] Y. Konishi, L.B. Yang, P. He, K. Lindholm, B. Lu, R. Li, et al., Deficiency of GDNF Receptor GFRalpha1 in Alzheimer's Neurons Results in Neuronal Death, J. Neurosci. 34 (2014) 13127–13138.
[52] S.M. Rocha, A.C. Cristovao, F.L. Campos, C.P. Fonseca, G. Baltazar, Astrocyte-derived GDNF is a potent inhibitor of microglial activation, Neurobiol. Dis. 47 (2012) 407–415.
[53] C. Iannotti, H. Li, P. Yan, X. Lu, L. Wirthlin, X.M. Xu, Glial cell line-derived neurotrophic factor-enriched bridging transplants promote propriospinal axonal regeneration and enhance myelination after spinal cord injury, Exp. Neurol. 183 (2003) 379–393.
[54] J. Jourquin, E. Tremblay, A. Bernard, G. Charton, F.A. Chaillan, E. Marchetti, et al., Tissue inhibitor of metalloproteinases-1 (TIMP-1) modulates neuronal death, axonal plasticity, and learning and memory, Eur. J. Neurosci. 22 (2005) 2569–2578.
[55] M. Niimura, N. Takagi, K. Takagi, R. Mizutani, K. Tanonaka, H. Funakoshi, et al., The protective effect of hepatocyte growth factor against cell death in the hippocampus after transient forebrain ischemia is related to the improvement of apurinic/apyrimidinic endonuclease/redox factor -1 level and inhibition of NADPH oxidase activity, Neurosci. Lett. (2006) 136–140.

[56] J.W. Li, L.L. Li, L.L. Chang, Z.Y. Wang, Y. Xu, Stem cell factor protects against neuronal apoptosis by activating AKT/ERK in diabetic mice, Braz. J. Med. Biol. Res. 42 (2009) 1044–1049.
[57] A. Fragkouli, E.C. Tsilibary, A.K. Tzinia, Neuroprotective role of MMP-9 overexpression in the brain of Alzheimer's 5xFAD mice, Neurobiol. Dis. 70 (2014) 179–189.
[58] J.M. Rubio-Perez, J.M. Morillas-Ruiz, A review: inflammatory process in Alzheimer's disease, role of cytokines, Sci. World J. 2012 (2012) 756357.
[59] C.K. Combs, Inflammation and microglia actions in Alzheimer's disease, J. Neuroimmune Pharmacol. 4 (2009) 380–388.
[60] H. Fujii, K. Matsubara, K. Sakai, M. Ito, K. Ohno, M. Ueda, et al., Dopaminergic differentiation of stem cells from human deciduous teeth and their therapeutic benefits for Parkinsonian rats, Brain Res. 1613 (2015) 59–72.
[61] R.G. Thorne, G.J. Pronk, V. Padmanabhan, W.H. Frey, 2nd, Delivery of insulin-like growth factor-I to the rat brain and spinal cord along olfactory and trigeminal pathways following intranasal administration, Neuroscience 127 (2004) 481–496.
[62] D. Gomez, J.A. Martinez, L.R. Hanson, W.H. Frey, 2nd, C.C. Toth, Intranasal treatment of neurodegenerative diseases and stroke, Front. Biosci. 4 (2012) 74–89.
[63] R.G. Thorne, G.J. Pronk, V. Padmanabhan, W.H. Frey, Delivery of insulin-like growth factor-I to the rat brain and spinal cord along olfactory and trigeminal pathways following intranasal administration, Neuroscience 127 (2004) 481–496.
[64] L.R. Hanson, W.H. Frey 2nd, Intranasal delivery bypasses the blood-brain barrier to target therapeutic agents to the central nervous system and treat neurodegenerative disease, BMC Neurosci. 9 (Suppl 3) (2008) S5.
[65] S. Capsoni, S. Marinelli, M. Ceci, D. Vignone, G. Amato, F. Malerba, et al., Intranasal painless human Nerve Growth Factors slows amyloid neurodegeneration and prevents memory deficits in App X PS1 mice, PloS One 7 (2012) e37555.
[66] W. Zhang, W. Zhang, Z. Li, J. Hao, Z. Zhang, L. Liu, et al., S14G-humanin improves cognitive deficits and reduces amyloid pathology in the middle-aged APPswe/PS1dE9 mice, Pharmacol. Biochem. Behav. 100 (2012) 361–369.